

A Low Energy Gap Organic Dye for High-Performance Small Molecule Organic Solar Cells

Li-Yen Lin,^a Yi-Hong Chen,^b Zheng-Yu Huang,^b Hao-Wu Lin,^{b*} Shu-Hua Chou,^a
Francis Lin,^a Chang-Wen Chen,^b Yi-Hung Liu,^a Ken-Tsung Wong^{a*}

^a Department of Chemistry, National Taiwan University, Taipei 10617, Taiwan

^b Department of Materials Science and Engineering, National Tsing Hua University,
Hsin Chu 30013, Taiwan

Supporting Information

Contents	page
Synthetic procedures	S2
Cyclic voltammetry measurement	S4
Quantum mechanical calculations	S5
Figure S1. Computed absorption spectrum of DTDCTB (oscillator strengths $f > 0.06$).	S5
Table S1. Calculated TDDFT Vertical Excitation Energies (eV, nm), Oscillator Strengths (f), Composition in Terms of Molecular Orbital Contributions, and Transition Characters	S6
Table S2. Isodensity Surface Plots and Calculated Energy Levels of the HOMO and LUMO of DTDCTB	S7
OPVs device fabrication and testing	S8
Device characteristics of DTDCTB:C ₆₀ PMHJ solar cells with different thicknesses of DTDCTB: Figure S2 and Table S3	S9
Device characteristics of DTDCTB:C ₇₀ PMHJ solar cells with different thicknesses of MoO ₃ : Figure S3 and Table S4	S10
Spectrum response modeling to extract exciton diffusion length of the DTDCTB thin film: Figure S4	S11
X-ray diffraction spectra of the DTDCTB and DTDCTB:C ₇₀ thin film: Figure S5	S12
Surface morphology of the DTDCTB:C ₇₀ (1:1, by volume) thin film: Figure S6	S13
¹ H and ¹³ C spectra	S14

Synthetic procedures:

General Methods: All chemicals and reagents were used as received from commercial sources without purification. Solvents for chemical synthesis were purified by distillation. All chemical reactions were carried out under an argon or nitrogen atmosphere.

Synthesis of 4-Bromo-7-dibromomethyl-2,1,3-benzothiadiazole (1). A mixture of 4-bromo-7-methyl-2,1,3-benzothiadiazole (45.82 g, 200 mmol), azobisisobutyronitrile (6.57 g, 40 mmol), and *N*-bromosuccinimide (106.2 g, 600 mmol) in chlorobenzene (400 mL) was stirred and heated at 80 °C for 4h. After cooling to room temperature, the reaction mixture was filtered to remove the solid succinimide, and then the filtrate was washed with water and brine, dried over anhydrous MgSO₄, and filtered. The solvent of the filtrate was removed by rotary evaporation, and the crude product was purified by column chromatography on silica gel with CH₂Cl₂/hexane (v/v, 1:3) as eluent to afford **1** as a white solid (56.1 g, 83%). M.p. 119-120 °C; IR (KBr) ν 3001, 2922, 1524, 1481, 1315, 1274, 1185, 1097, 937, 880 cm⁻¹; ¹H NMR (CDCl₃, 400 MHz) δ 7.97-7.90 (m, 2H), 7.40 (s, 1H); ¹³C NMR (CDCl₃, 100 MHz) δ 152.8, 149.6, 133.4, 131.8, 129.4, 115.8, 33.9; HRMS (m/z, FAB⁺) Calcd for C₇H₃⁷⁹Br₃N₂S 383.7567, found 383.7542, Calcd for C₇H₃⁷⁹Br₂⁸¹BrN₂S 385.7547, found 385.7553, Calcd for C₇H₃⁷⁹Br₁⁸¹Br₂N₂S 387.7526, found 387.7524, Calcd for C₇H₃⁸¹Br₃N₂S 389.7506, found 389.7536.

Synthesis of 7-Bromo-2,1,3-benzothiadiazole-4-carbaldehyde (2). To a stirring solution of **1** (260 mg, 0.67 mmol) in acetonitrile (8 mL) was added silver nitrate aqueous solution (285 mg, 1.68 mmol, water 1.7 mL) and then heated to reflux for 2h. After cooling to room temperature, the reaction mixture was filtered to remove the AgBr precipitate, and the filtrate was then extracted with CH₂Cl₂. The combined extracts were washed with brine, dried over anhydrous MgSO₄, and filtered. The solvent of the extracts was removed by rotary evaporation to afford **2** as a white solid (147 mg, 92%). M.p. 185-186 °C; IR (KBr) ν 3078, 3021, 2835, 2728, 1702, 1526, 1268, 1102, 937, 879 cm⁻¹; ¹H NMR (CDCl₃, 400 MHz) δ 10.71 (s, 1H), 8.09-8.03 (m, 2H); ¹³C NMR (CDCl₃, 100 MHz) δ 188.0, 153.8, 152.1, 131.9, 131.5, 126.7, 121.7; HRMS (m/z, FAB⁺) Calcd for C₇H₃⁷⁹BrN₂OS 241.9149, found 241.9149, Calcd for C₇H₃⁸¹BrN₂OS 243.9129, found 243.9137.

Synthesis of 4-Bromo-7-dicyanovinyl-2,1,3-benzothiadiazole (3). A mixture of **2** (150 mg, 0.62 mmol), malononitrile (82 mg, 1.24 mmol), and basic aluminum oxide (310 mg) in anhydrous toluene (7 mL) was stirred and heated at 70 °C for 2h. After the reaction mixture was cooled to room temperature, the basic aluminum oxide residue was removed by filtration and thoroughly washed with toluene. The solvent of the filtrate was removed by rotary evaporation, and the crude product was purified by

column chromatography on silica gel with CH₂Cl₂/hexane (v/v, 1:1) as eluent to afford **3** as a yellow solid (120 mg, 67%). M.p. 179-180 °C; IR (KBr) ν 3097, 3032, 2229, 1573, 1517, 1380, 1126, 1044, 933, 884 cm⁻¹; ¹H NMR (CDCl₃, 400 MHz) δ 8.73 (s, 1H), 8.53 (d, *J* = 7.6 Hz, 1H), 8.05 (d, *J* = 7.6 Hz, 1H); ¹³C NMR (CDCl₃, 100 MHz) δ 153.0, 152.5, 152.2, 132.0, 130.0, 123.0, 121.8, 113.1, 112.3, 85.2; HRMS (m/z, FAB⁺) Calcd for C₁₀H₃⁷⁹BrN₄S 289.9262, found 289.9263, Calcd for C₁₀H₃⁸¹BrN₄S 291.9241, found 291.9237.

Synthesis of 2-{[7-(5-*N,N*-ditolylaminothiophen-2-yl)-2,1,3-benzothiadiazol-4-yl]methylene}malononitrile (DTDCTB). A mixture of **3** (1.46 g, 5 mmol), 5-(*N,N*-ditolylamino)-2-(tri-*n*-butylstannyl)thiophene (3.55 g, 6.25 mmol), and PdCl₂(PPh₃)₂ (175 mg, 0.25 mmol) in anhydrous toluene (25 mL) was stirred and heated at 110 °C under argon for 2h. After the reaction mixture was cooled to room temperature, the solvent was removed by rotary evaporation, and the crude product was purified by column chromatography on silica gel with CH₂Cl₂/hexane (v/v, 1:1) as eluent to afford **DTDCTB** as a black solid (1.34, 55%). M.p. 234 °C (DSC); IR (KBr) ν 3033, 2917, 2217, 1566, 1454, 1329, 1265, 1153, 1062, 921, 827 cm⁻¹; ¹H NMR (CDCl₃, 400 MHz) δ 8.66 (s, 1H), 8.60 (d, *J* = 8.0 Hz, 1H), 8.22 (d, *J* = 4.4 Hz, 1H), 7.57 (d, *J* = 8.0 Hz, 1H), 7.22-7.17 (m, 8H), 6.50 (d, *J* = 4.4 Hz, 1H), 2.39 (s, 6H); ¹³C NMR (CDCl₃, 100 MHz) δ 161.0, 154.6, 151.5, 150.6, 143.8, 135.5, 134.0, 133.2, 130.8, 130.2, 126.0, 124.9, 120.9, 118.9, 114.6, 114.3, 113.8, 78.5, 21.1; HRMS (m/z, FAB⁺) Calcd for C₂₈H₁₉N₅S₂ 489.1082, found 489.1083.

Cyclic voltammetry measurement:

The electrochemical properties of **DTDCTB** were investigated by cyclic voltammetry (CV). The oxidation potentials were carried out in anhydrous CH_2Cl_2 solution (1.0 mM) containing 0.1 M tetra-*n*-butylammonium hexafluorophosphate (TBAPF_6) as a supporting electrolyte, and the reduction potentials were measured in anhydrous THF solution (1.0 mM) containing 0.1 M tetra-*n*-butylammonium perchlorate (TBAP) as a supporting electrolyte, purged with argon prior to conduct the experiments. A glassy carbon electrode and a platinum wire were used as the working and counter electrodes, respectively. All potentials were recorded versus Ag/AgCl (saturated) as a reference electrode and calibrated with the ferrocene/ferrocenium redox couple. All measurements were performed at a scan rate of 100 mV s^{-1} .

Quantum mechanical calculations:

The electronic and optical properties of **DTDCTB** have been estimated by density functional theory (DFT) and time-dependent DFT (TDDFT) calculations in CH_2Cl_2 solution using hybrid B3LYP function with the 6-31G(d) basis set, as implemented in the Gaussian09 (G09) program package.¹ The first electronic transition corresponds to a charge-transfer (CT) excitation from the ditolylaminothieny-localized HOMO to the LUMO, which is sizably populated on 2,1,3-benzothiadiazole and dicyanovinylene moieties (Table S1~2). The excitation energy of this lowest transition with the largest oscillator strength is calculated to be 1.84 eV (673.2 nm) (Figure S1), which is close to the observed experimental results. The second and third transitions may stem from two different $\pi \rightarrow \pi^*$ excitations from the HOMO-1 to the LUMO and from the HOMO to the LUMO+1.

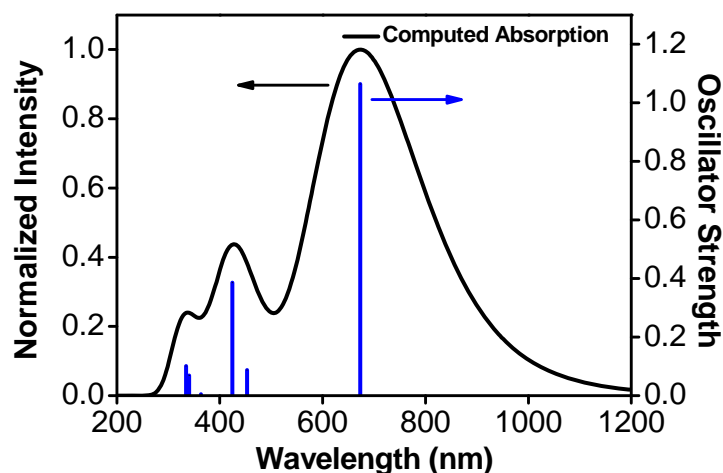


Figure S1. Computed absorption spectrum of **DTDCTB** (oscillator strengths $f > 0.06$).

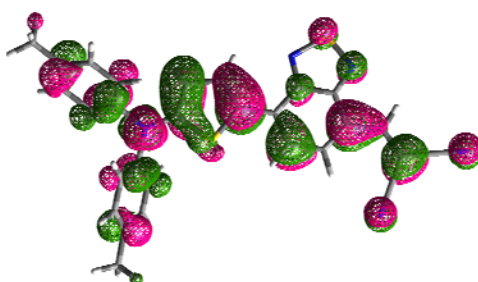
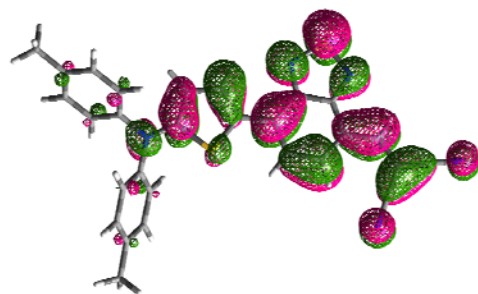
¹ Censo, D. D.; Fantacci, S.; Angelis, F. D.; Klein, C.; Evans, N.; Kalyanasundaram, K.; Bolink, H. J.; Grätzel, M.; Nazeeruddin, M. K. *Inorg. Chem.* **2008**, 47, 980.

Table S1. Calculated TDDFT Vertical Excitation Energies (eV, nm), Oscillator Strengths (f), Composition in Terms of Molecular Orbital Contributions, and Transition Characters^a

<i>Electronic Transition</i>	<i>E (eV, nm)</i>	<i>f</i>	Composition	Character
$S0 \rightarrow S1$	1.84 (673.2)	1.06	70% HOMO \rightarrow LUMO	charge-transfer
$S0 \rightarrow S2$	2.74 (454.2)	0.09	42% HOMO-1 \rightarrow LUMO, 56% HOMO \rightarrow LUMO+1	$\pi \rightarrow \pi^*$
$S0 \rightarrow S3$	2.92 (424.4)	0.39	56% HOMO \rightarrow LUMO+1, 41% HOMO-1 \rightarrow LUMO	$\pi \rightarrow \pi^*$

^a Within the considered energy range, we selectively calculate three transitions with moderate intensity ($f > 0.09$).

Table S2. Isodensity Surface Plots and Calculated Energy Levels of the HOMO and LUMO of DTDCTB

Orbital	Isodensity Surface Plot	Energy Level (eV)
HOMO		5.14
LUMO		3.13

OPVs device fabrication and testing:

Organic compounds including the synthesized **DTDCTB**, purchased fullerene C_{60} (C_{70}), and 2,9-Dimethyl-4,7-Diphenyl-1,10-Phenanthroline (BCP) were subject to purification at least once by temperature-gradient sublimation before use in this study. The organic and metal oxide thin films and metal electrodes were deposited on indium tin oxide (ITO) coated glass substrates in a high vacuum chamber with base pressure $\sim 1 \times 10^{-6}$ Torr. The sheet resistance of ITO is $\sim 15 \Omega/\text{sq}$. The deposition was performed at a rate of 2-3 Å with the substrate held at room temperature. Thicknesses were monitored using a crystal oscillator during deposition and were verified later with spectroscopic ellipsometry. The active area of the cells had an average size of 2.5-5 mm². Devices were encapsulated using a UV-cured sealant (*Everwilde Chemical Co., Epowide EX*) and a cover glass under the dry nitrogen atmosphere after fabrication and were measured in air. Current density-voltage characteristics were measured with a SourceMeter *Keithley* 2636A under illumination of AM1.5G solar light from a xenon lamp solar simulator (*Abet Technologies*). The incident light intensity was calibrated as 100 mW/cm². The external quantum efficiency spectra were taken by illuminating chopped monochromatic light with a continuous-wave bias white light (from halogen lamp) on the solar cells. The photocurrent signals were extracted with lock-in technique using a current preamplifier (*Stanford Research System*) followed by a lock-in amplifier (*AMETEK*). The EQE measurement is fully computer controlled and the intensity of monochromatic light is carefully calibrated with optical power meter (*Ophir Optronics*). Absorption spectra were acquired with spectrometer (*PerkinElmer*). Organic films for photoelectron spectroscopy and ellipsometry measurements were vacuum deposited on fused silica substrates. The HOMO values of thin films were acquired with a photoelectron spectrometer (*Riken Keiki Co. Ltd.*). Ellipsometry measurements were carried out with *J. A. Woollam Inc.* V-VASE variable-angle spectroscopic ellipsometer. Simulation program is coded with *Matlab* software (*The MathWorks, Inc.*) and performed with dual-core *Intel*-CPU personal computer. Atomic force microscopy (AFM) images were taken with *Veeco Nanoscope 3100* atomic force microscope. The film preparation conditions for the AFM measurements were kept the same as device fabrication for accurate comparison.

Device characteristics of DTDCTB:C₆₀ PMHJ solar cells with different thicknesses of DTDCTB:

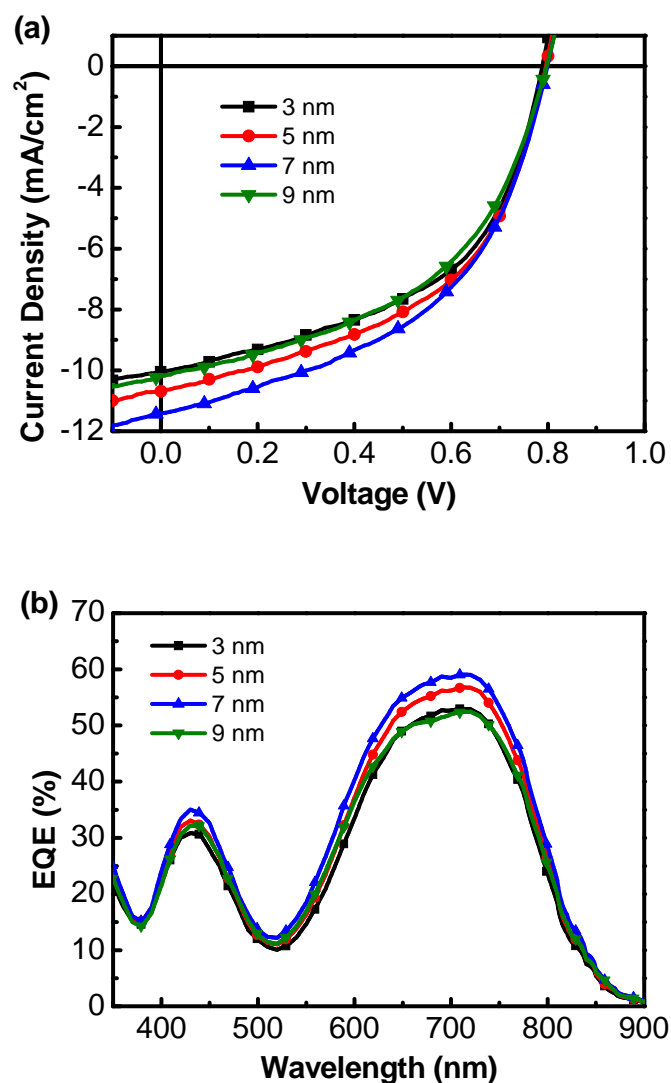


Fig. S2 (a) J-V characteristics and (b) EQE spectra of **DTDCTB:C₆₀** PMHJ solar cells. The device structures are: ITO/MoO₃ (30 nm)/**DTDCTB** (3, 5, 7, 9 nm)/**DTDCTB:C₆₀** (1:1, 40 nm)/C₆₀ (20 nm)/BCP (10 nm)/Ag (150 nm).

TABLE S3. Performance Parameters of Devices

Device	V _{oc} (V)	J _{sc} (mA/cm ²)	Integrated EQE (mA/cm ²)	FF	η _{PCE} (%)
3 nm	0.79	10.04	9.53	0.51	4.02
5 nm	0.80	10.68	10.30	0.50	4.11
7 nm	0.80	11.40	10.97	0.48	4.41
9 nm	0.80	10.20	9.84	0.48	3.91

Device characteristics of DTDCTB:C₇₀ PMHJ solar cells with different thicknesses of MoO₃:

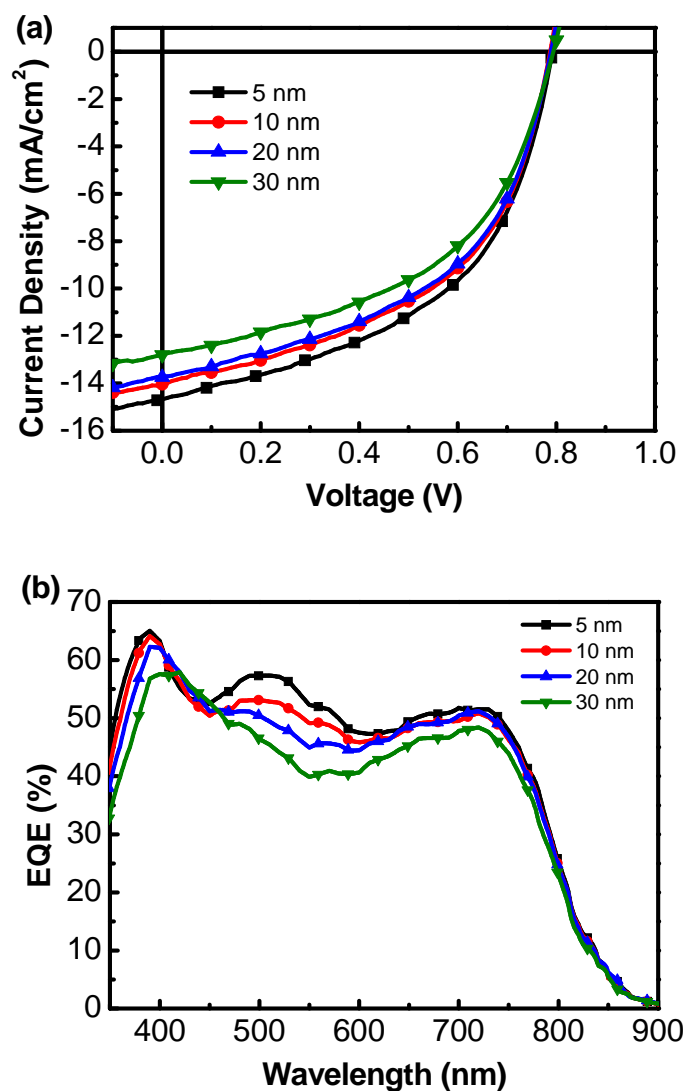


Fig. S3 (a) J-V characteristics and (b) EQE spectra of **DTDCTB:C₇₀** PMHJ solar cells. The device structures are: ITO/MoO₃ (5, 10, 20, 30 nm)/**DTDCTB** (7 nm)/**DTDCTB:C₇₀** (1:1, 40 nm)/C₇₀ (7 nm)/BCP (10 nm)/Ag (150 nm).

TABLE S4. Performance Parameters of Devices

Device	V _{oc} (V)	J _{sc} (mA/cm ²)	Integrated EQE (mA/cm ²)	FF	η _{PCE} (%)
5 nm	0.79	14.68	14.26	0.50	5.81
10 nm	0.79	14.00	13.71	0.50	5.50
20 nm	0.79	13.74	13.46	0.50	5.41
30 nm	0.79	12.80	12.56	0.49	4.98

Spectrum response modeling to extract exciton diffusion length of the DTDCTB thin film:

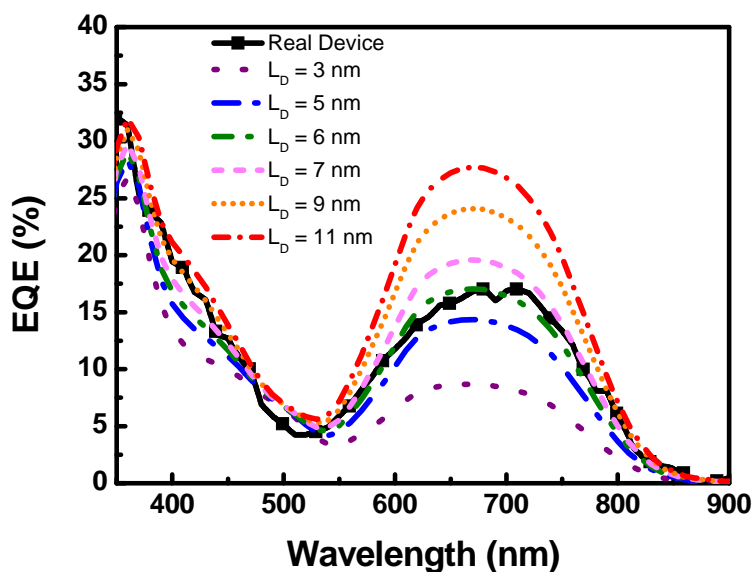


Fig. S4 The measured EQE spectrum of the **DTDCTB**/ C_{60} bilayer device and modeled spectra with various exciton diffusion lengths (L_D) of the **DTDCTB** thin film. The device structure is: ITO/MoO₃ (30 nm)/**DTDCTB** (15 nm)/ C_{60} (5 nm)/BCP (10 nm)/Ag (150 nm).

For detailed measurement and modeling procedures, please refer to [Pettersson, L. A. A.; Roman, L. S.; Inganäs, O. *J. Appl. Phys.* **1999**, 86, 487]. The optical constants of thin films used in the transfer matrix modeling were taken by spectroscopic ellipsometer. The modeled EQE with $L_D = 6$ nm agrees well with the experimental data. The results indicate the exciton diffusion length of the **DTDCTB** thin film is about 6 nm.

X-ray diffraction spectra of the DTDCTB and DTDCTB:C₇₀ thin film:

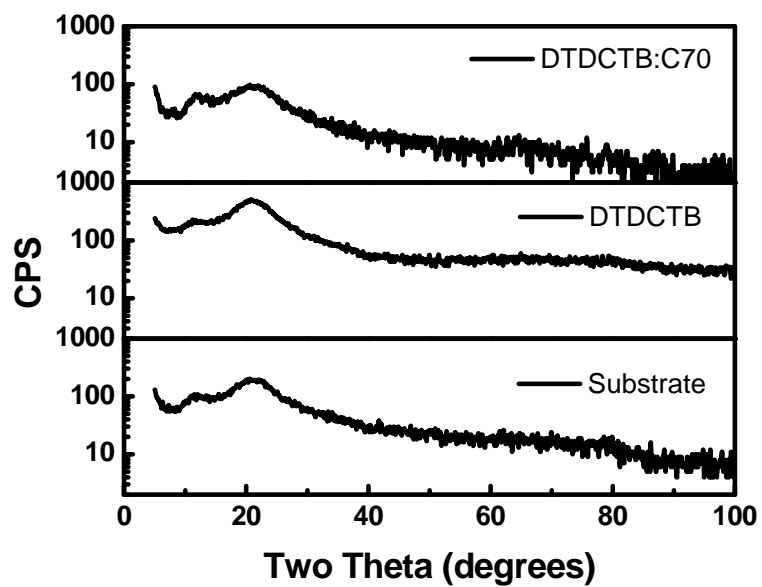


Fig. S5 X-ray diffractograms of the **DTDCTB** and **DTDCTB:C₇₀** (1:1) thin film on a fused silica substrate.

Surface morphology of the DTDCTB:C₇₀ (1:1, by volume) thin film:

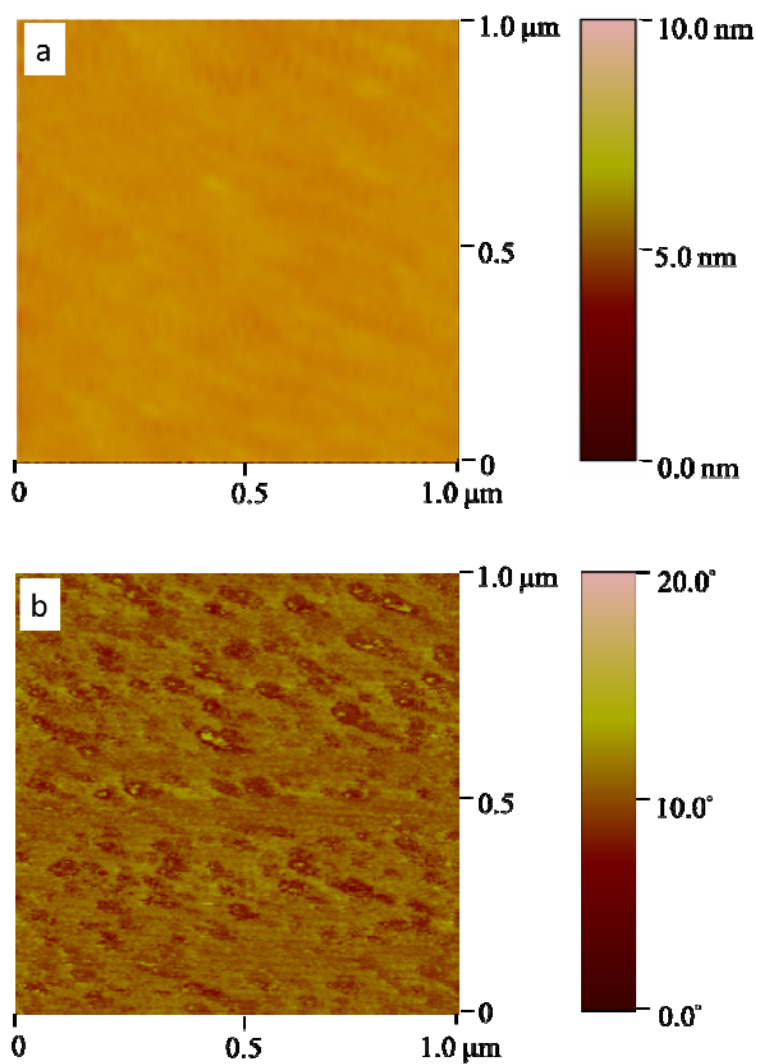


Fig. S6 (a) AFM topographic image and (b) phase image of the **DTDCTB:C₇₀** mixed layer, as showed in a 1 μm × 1 μm surface area.

